International Journal of Mass Spectrometry 463 (2021) 116548

Contents lists available at ScienceDirect

International Journal of Mass Spectrometry

journal homepage: www.elsevier.com/locate/ijms

Gas-phase dissociation pathways of Beta-2 agonists

Matthew J. Carlo [a], Peyton M. York [b], Amanda L. Patrick [a, *]

[a] Department of Chemistry, Mississippi State University, Mississippi State, MS, 39762, USA
[b] Department of Biochemistry, Mississippi State University, Mississippi State, MS, 39762, USA

ARTICLE INFO

Article history:
Received 21 December 2020
Received in revised form
7 February 2021
Accepted 8 February 2021
Available online 14 February 2021

Keywords:
Performance-enhancing drugs
DFT
CID-MS
Unimolecular dissociation

ABSTRACT

Beta-2 agonists are widely used for the treatment of asthma and other respiratory conditions. These same drugs, however, may also be taken with the aim of gaining an unfair advantage in sports competition, thus they are controlled under anti-doping initiatives. While there are several analytical protocols relying on MS/MS to identify various molecules in this class, relatively little work has been done on unraveling the underlying gas-phase dissociation chemistry for this class of molecules. Here, we apply collision-induced dissociation mass spectrometry (CID-MS) to a group of beta-2 agonists to explore characteristic dissociation pathways and we perform complementary density functional theory calculations to better understand the underlying chemistry and the associated theoretical thermodynamics. Common dissociation pathways include one or more losses of water, and cleavage at the amine nitrogen is common, sometimes with the observance of complementary charge-retention pairs. In the case of more complex molecules, additional losses are observed, which lend insights into their specific structures. These various pathways are discussed in detail for protonated isoetharine, salbutamol, formoterol, and salmeterol. The goal of this work is to contribute to a foundation of knowledge on the dissociation pathways of pharmaceuticals, especially those regulated as performance enhancing drugs.

1. Introduction

Beta-2 agonists are a class of drugs commonly used to treat respiratory conditions, including asthma [1–3]. In addition to their well-established role in the medical realm, this class of drugs is also banned and/or regulated under sports anti-doping initiatives, due to their potential for abuse as performance-enhancing drugs [4–6]. As such, they make an appearance on the list of banned and controlled substances published by the World Anti-Doping Agency (WADA) [7]. Given the history and importance of beta-2 agonists, many studies including those implementing LC-MS/MS detection have been undertaken, with several focused on human sample (urine, plasma, etc.) analysis [8–13]. While the specific motivations of each study differs, in general these results and methods are useful for areas as diverse as understanding drug metabolism, monitoring clinical use of the pharmaceutical, and screening for sports doping violations. Various other studies have focused on analysis of beta-2 agonists in animals, food, and feed [14–16] and environmental and wastewater monitoring of pharmaceuticals, drugs of abuse, and lifestyle drugs (often including beta-2 agonists) is an emerging field [17–21]. Such studies can be useful both for determining the extent to which specific pharmaceuticals serve as environmental contaminants and for monitoring population-scale drug use and/or abuse.

Within MS/MS analyses, diagnostic ions are typically used for characterization and quantitation of the analyte(s) of interest, here beta-2 agonists. However, a cursory report of tentative neutral loss assignments are, at most, the only information reported [11,15,16]. In one study the authors proposed a structure for a diagnostic product ion (m/z 148); however, complementary calculations or confirmatory structural experiments were not reported therein [12]. And yet, it is clear that fundamental understandings of gas-phase dissociation pathways is useful toward improved screening methodologies [22,23] and such investigations serve basic science well.

While beta-2 agonists specifically have not yet been the subject of in-depth mapping of gas-phase unimolecular dissociation pathways, of course, a vast literature exists examining mechanisms associated with various structural motifs. Given that water loss, potentially from any one of several hydroxyl groups, is known to be a typical dissociation path and that there is a substituted benzyl group in all of the analyte structures, the historical literature on

* Corresponding author.
E-mail address: apatrick@chemistry.msstate.edu (A.L. Patrick).

https://doi.org/10.1016/j.ijms.2021.116548
1387-3806/

alcohol dissociation pathways [24,25] and tropylium ion formation [26–28] was especially influential to the current study. Of specific relevance, a study including deuterium labeling of 3-hydroxy steroids suggests that the axial 3α-hydroxyl functional group loses water solely through 1,3 elimination, whereas the 3β-hydroxyl functional group seems to dissociate via more diverse mechanisms [25]. These studies inform our initial considerations of the water loss mechanisms throughout the current study.

Here, we report energy-resolved collision-induced dissociation (CID) mass spectra of four beta-2 agonists, (isoetharine, salbutamol, formoterol, and salmeterol), proposed dissociation pathways (including evaluation of competing pathways/mechanisms where appropriate), and theoretical thermodynamics obtained through DFT calculations. We specifically focus on finding common patterns between the different analyte species, better understanding the relationship between (e.g., competitive vs sequential) observed product ions, and gaining insights into thermodynamically preferred ion structures when multiple potential mechanisms for a given neutral loss can be hypothesized. As an aside, we comment on the utility of MS/MS in differentiating between structural isomers (isoetharine and salbutamol).

2. Materials and methods

2.1. Sample preparation

Salbutamol, formoterol fumarate, and salmeterol were purchased from Santa Cruz Biotechnology (Dallas, TX) and isoetharine mesylate was purchased from Sigma-Aldrich (St Louis, MO). HPLC-grade methanol and glacial acetic acid were purchased from Fisher Scientific (Waltham, MA). All chemicals were used as purchased. Typically, solutions were prepared of each individual analyte, with concentrations of ~5 ppm in each final spray solution diluted in a solvent of 99.5% methanol and 0.5% acetic acid added.

2.2. Mass spectrometry

MS/MS spectra were collected using a Bruker microTOF-Q II mass spectrometer equipped with an electrospray ionization source (Billerica, MA). Spray solutions were introduced into the electrospray source at a rate of 5 μL/min using a KD Scientific syringe pump (Holliston, MA). All experiments were performed in the positive mode. Typical source conditions include transfer capillary temperature of 180 °C, capillary voltage of 4500 V, offset of −500 V, nitrogen gas flow of 1.6 L/min, collision cell RF amplitude of 100 V_{pp}, and transfer time of 85.0 μs. Other parameters were tuned appropriately for ion transmission. Note that transmission of low mass fragment ions is reliant upon a low(er) setting of the RF amplitude applied to the collision cell.

Energy-resolved CID-MS were collected for the protonated precursor of each analyte. Briefly, the precursor ion was mass selected with an isolation width typically set to 3.0 u using the quadrupole mass filter, the ions were then subjected to CID (with variable collision energy starting at 0 eV and progressing in 1 eV steps), and the resulting product ions and remaining precursor ions were measured at each energy step using the ToF mass analyzer. Each data point corresponds to 120 spectra collected at a rate of 2 scans per second, averaged, and analyzed using Equation (1). Energy-resolved CID curves are plotted as percent yield versus collision energy, where percent yield is given by Equation (1),

$$\%\ \text{Yield} = \left(\frac{I_{F1}}{I_P + \sum I_F}\right) \times 100 \qquad \text{Equation 1}$$

where I_{F1} is the integral intensity of the product ion of interest, I_P is the integral intensity of the remaining precursor ion, and $\sum I_F$ is the sum of integral intensities of all of the fragment ions. In each case, the precursor ion depletion is also plotted for reference, in which case I_{F1} is replaced with I_P in Equation (1). Representative annotated mass spectra at specific collision energies are available in the accompanying Supporting Information.

MS^n spectra were collected using a Thermo LTQ-XL ion trap mass spectrometer (San Jose, CA). Samples were introduced to the mass spectrometer via an Excellims MA-3100 ion mobility spectrometer (Acton, MA) operated in the open mode, with an electrospray ionization source. Typical source conditions include a source voltage of 1.8 kV, drift tube voltage of 10 kV, and drift tube temperature of 180 °C. Other parameters were tuned as needed. Mass selection and collision energy details are provided with the data (see Figures S3, S6, S7, S9, S10, S11, S12).

2.3. Computational chemistry

Starting structures of protonated precursor ions, fragment ions, and neutral losses were drawn using Avogadro 1.2.0 [29] and Gabedit [30] was used to generate a large number of candidate conformations for each ion. Each produced conformer was then submitted to Gaussian 16 [31] for geometry optimization, frequency calculations, and thermodynamic calculations at the B3LYP/6−311++G** level of theory. Each output file was checked to insure there were no imaginary frequencies. For each unique structure, the lowest energy conformer was selected for further use in thermodynamic calculations for the relevant reaction pathways. Coordinates for the lowest-energy conformer of each species are available in the Supporting Information.

3. Results and discussion

3.1. CID-MS based differentiation of the structural isomers salbutamol and isoetharine

Before delving into the specifics of dissociation pathways, it is worth first looking at the dissociation patterns of the two structural isomers of the set, salbutamol and isoetharine. The structures of these two molecules are provided in Fig. 1. Isoetharine terminates in a propyl-substituted amine, has an ethyl side-group, and has two phenolic OH groups. Salbutamol, on the other hand, terminates in a tert-butyl-substituted amine, has no additional alkyl groups, and has one phenolic OH and one hydroxymethyl group on the aromatic ring. Given that the two compounds are isomeric, electrospray mass spectrometry alone fails to distinguish between them, with each having a protonated pseudo-molecular ion at *m/z* 240.

Upon CID (Fig. 1), differentiation is straightforward. While both salbutamol and isoetharine first lose 18 u to produce a first product ion at *m/z* 222, the similarities in the CID-MS spectra stop there. The next loss, with product ions appearing at *m/z* 166 And *m/z* 180 for salbutamol and isoetharine, respectively. This set of product ions can tentatively be assigned to the loss of the terminating alkyl group (circled for each structure), providing structural insights into the individual isomers. From there, salbutamol has a third prominent product ion, at *m/z* 148, whereas isoetharine does not. Together, these two differences in MS/MS pattern are sufficient for confident differentiation of the two isomers. The proceeding sections will discuss why the dissociation patterns appear as they do for each molecule.

3.2. Mapping dissociation pathways

3.2.1. Isoetharine

Isoetharine is a typical beta-2 agonist, with a relatively simple

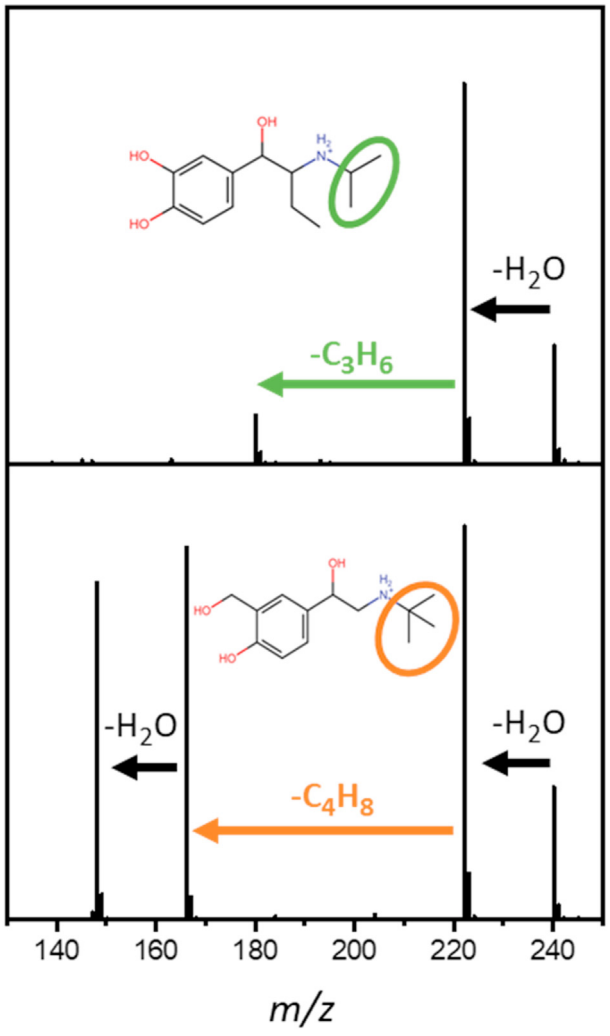

Fig. 1. CID-MS of (top) protonated isoetharine (10 eV collision energy) and (bottom) protonated salbutamol (10 eV collision energy). A key difference in the spectra, the nature of the hydrocarbon loss, is highlighted both in the neutral loss assignments and on the molecular structures.

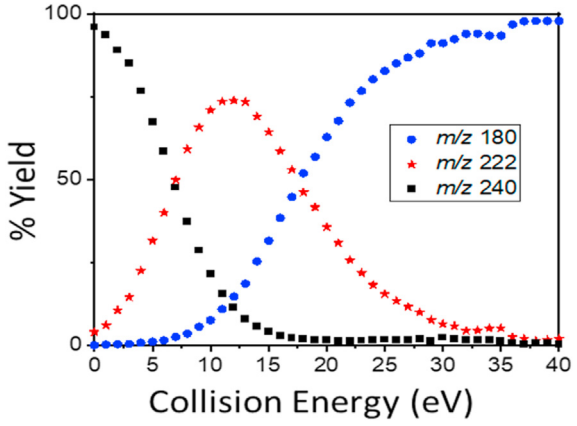

Fig. 2. Energy-resolved CID of protonated isoetharine. Black squares represent the precursor ion (m/z 240), red stars represent the m/z 222 product ion, and blue circles represent the m/z 180 product ion.

structure. The energy-resolved CID data for protonated isoetharine is provided in Fig. 2 and a summary of proposed dissociation pathways, with structures and theoretical enthalpies, is illustrated in Fig. 3.

As illustrated in Fig. 2, there are only two significant dissociation pathways. The first, producing a product ion at *m/z* 222 (red stars), corresponds to a nominal neutral loss of 18 u, which can be assigned to water loss. The other observed product ion appears at *m/z* 180 (blue circles), representing a neutral loss of 60 u (or consecutive loss of 42 u from the *m/z* 222 fragment ion). This pathway can be assigned to the loss of water followed by the consecutive loss of the terminal propyl group. The shapes of the energy-resolved curves appear to be consistent with a sequential mechanism of formation of the *m/z* 180 ion, as the intensity of the *m/z* 222 ion begins to deplete in the same energy region as the *m/z* 180 ion begins to increase. The assignment as sequential is corroborated by MS^2 and MS^3 spectra collected using an ion trap mass spectrometer (Figure S3).

It has been shown in the literature that beta-2 agonists containing the characteristic ethanolamine side chain and terminating with a *tert*-butyl or isopentyl group will yield product ions at *m/z* 57 and 71 respectively [13]. In the case of isoetharine, the corresponding product ion would hypothetically appear at *m/z* 43. While we did not detect this ion in the current study, that may be due to the instrument rather than the chemistry.

Notably, loss of multiple water molecules is not observed from isoetharine, so phenolic groups can be ruled out as likely sites of water loss, leaving only the aliphatic alcohol as an active site for water loss, leading to the *m/z* 222 product ion. Water loss at this site

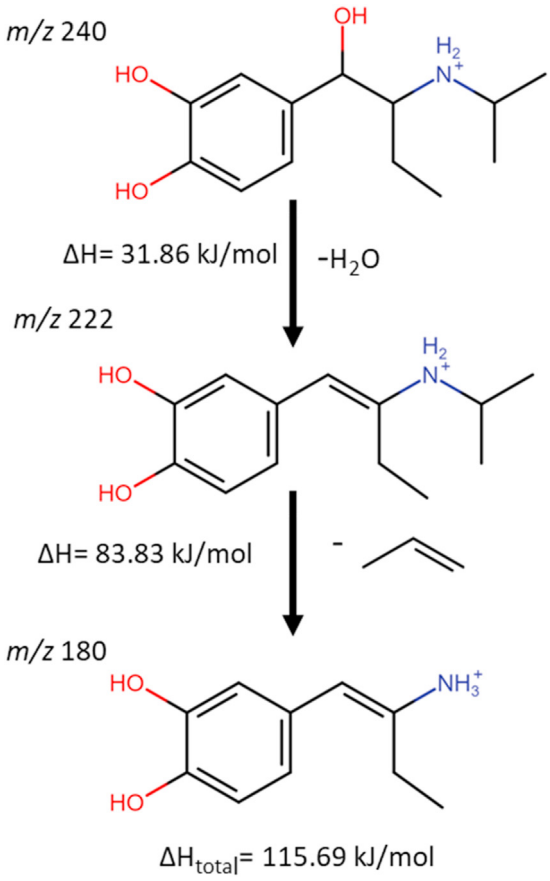

Fig. 3. Proposed lowest energy fragmentation pathway of isoetharine, with corresponding mass-to-charge ratios and theoretical thermodynamics.

could proceed via 1,2-elimination or 1,3-elimination (see Fig. 3 and Figure S18). For the 1,3- case, the resulting 3-membered ring could contain only carbon or could include a nitrogen. It was found that 1,3 elimination to form a nitrogen-containing ring was approximately 70 kJ/mol higher in energy than the 1,2-elimination case, and the path to form a carbon-only 3-membered ring was higher still. Thus, the 1,2-elimination pathway was assigned as the thermodynamically favorable pathway and was used as the starting point for consideration of sequential dissociation pathways. The sequential loss of the propyl group from the *m/z* 222 product ion, to form the *m/z* 180 product ion, is then calculated to have an associated enthalpy change of 83.83 kJ/mol (Fig. 3).

Direct formation of the propyl cation from the precursor ion (without associated water loss) was considered for theoretical energetic calculations, as illustrated in Figure S15. While we did not observe this product ion experimentally, similar pathways have been noted for other beta-2 agonists in the literature, so we performed theoretical calculations for completeness' sake. This pathway is calculated to have an associated enthalpy change of 272.35 kJ/mol, which is much less favorable than the observed successive losses of water and the isopropyl group and, thus, consistent with the experimental observations. The hypothetical product ion corresponding to charge-retention by the isopropyl group formed as a sequential dissociation product from the initial water loss ion, discussed above, was also considered as an alternative route to the hypothetical *m/z* 43 ion. Figure S16 illustrates this pathway; the associated enthalpy change was determined to be 229.33 kJ/mol. Thus, this pathway is not very favorable and, if it ever is active, it would only be expected at quite high collision energies and would, likely, produce a rather small intensity.

Finally, direct neutral loss of the propyl group (lost as propene) from the precursor ion, also not observed experimentally, was considered for theoretical energetic calculations. The hypothetical pathway is illustrated in Figure S17. The associated enthalpy change was determined to be 76.22 kJ/mol, which is considerably less favorable than initial water loss, which is consistent with the lack of experimental observance of this hypothetical fragmentation pathway.

3.2.2. Salbutamol

Salbutamol (also known as albuterol) is a very common beta-2 agonist and is a structural isomer of isoetharine (as discussed in Section 3.1). The energy-resolved CID curve for protonated salbutamol is shown in Fig. 4 and the proposed dissociation pathways are provided in Fig. 5.

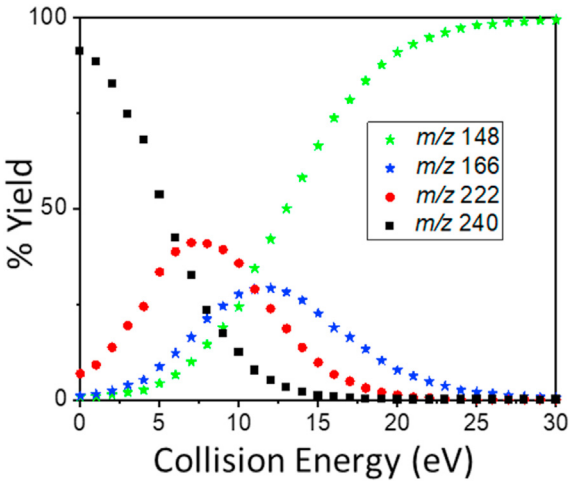

Fig. 4. Energy-resolved CID of protonated salbutamol. Black squares represent the precursor ion (m/z 240), red circles represent the m/z 222 product ion, blue stars represent the m/z 166 product ion, and green stars represent the m/z 148 product ion.

Considering Fig. 4, an initial product ion observed at *m/z* 222 (red circles), corresponding to loss of water—the same initial pathway as was observed for protonated isoetharine. The next highest mass product ion is observed at *m/z* 166 (blue stars), corresponding to a nominal neutral loss of 74 u from the precursor, or a 56 u sequential neutral loss from the *m/z* 222 product ion; this can be assigned as C—N bond cleavage at the terminal tert-butyl group, again in agreement with observations from isoetharine. Observance of the loss of the isobutene group is also in agreement with studies performed on non-deuterated and deuterated clenbuterol, a beta- 2 agonist also containing a terminal *tert*-butyl group [13]. A loss of 56 u for non-deuterated clenbuterol and losses of either 62 u or 63 u for deuterated clenbuterol are observed, which is consistent with our assignment of the 56 u loss here for salbutamol. The final major product ion is observed at *m/z* 148 (green stars), with a nominal neutral loss of 92 u from the precursor ion, or neutral loss of 18 u from the *m/z* 166 product ion, which can be assigned as additional water loss from that product ion.

Upon comparing the structures of isoetharine with salbutamol, the ability of salbutamol to undergo abundant loss of a second water molecule is likely due to the fact that isoetharine contains two phenolic OH groups, whereas salbutamol contains one phenolic OH group and one hydroxymethyl OH group, which is postulated to be the site of the second water loss. Strikingly, the curves for *m/z* 148 and *m/z* 166 turn on at nearly the same energies and appear to be either competitive or, if sequential, the *m/z* 148 product ion formation would be expected to be very energetically favorable. Complementary MS^n spectra (Figure S7) support the assignment of these pathways as sequential.

Given that salbutamol eventually loses two water molecules, it is not immediately clear in which order the hydroxyl groups will be lost, nor what mechanisms will be thermodynamically favorable. Fig. 5A shows the considered primary water loss mechanisms. In Pathway i, a tropylium ion is formed after loss of water from a methylhydroxyl group substituted on the aromatic ring. The enthalpy change associated with this reaction is 112.47 kJ/mol. Pathway ii considers loss of water from the backbone hydroxyl group, where water loss proceeds through β-elimination to form a double bond. The associated enthalpy change is 36.13 kJ/mol. Pathway iii is based on a product ion structure previously reported in the literature, resulting in the formation of an oxetane group after loss of water from the methylhydroxyl group, as the proton from the phenolic OH facilitates the water loss in this pathway and a C—O bond is formed. The enthalpy change associated with this reaction is 140.04 kJ/mol. Finally, pathway iv illustrates 1,3 elimination of water from the backbone hydroxyl group, with the formation of an aziridine moiety. This pathway was found to have a theoretical reaction enthalpy of 81.12 kJ/mol. Of the considered pathways, pathway ii is the most thermodynamically favorable pathway for primary neutral loss of water from protonated salbutamol. Thus, the product ion resulting from this pathway was the starting for further calculations of sequential neutral losses.

Fig. 5B shows the full proposed sequential fragmentation pathways of salbutamol, with calculated theoretical enthalpies for the most favorable product ion structures considered. The pathway initiates by β-elimination of water, resulting in C—C double bond formation. Then, cleavage of the C—N bond at the tert-butyl group is postulated, with abstraction of a hydrogen, retaining the charge on the amine group. This fragmentation step was found to have a theoretical reaction enthalpy of 91.90 kJ/mol. Finally, the pathway terminates with loss of a second water molecule, hypothetically through protonation of the methylhydroxyl OH followed by

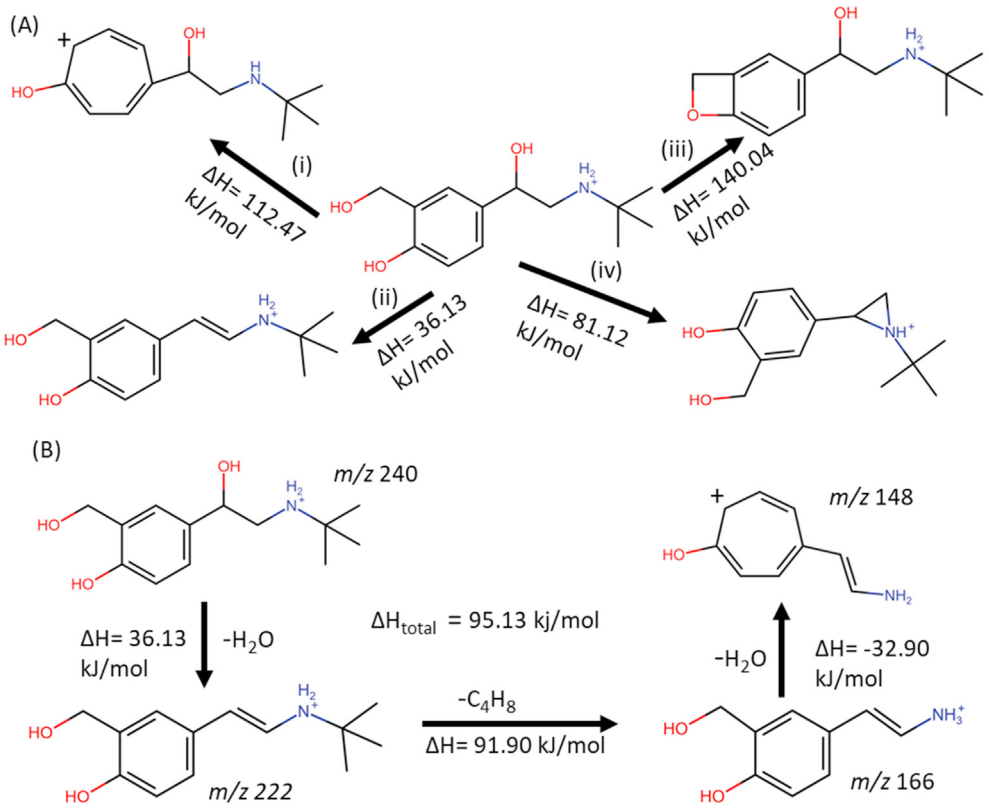

Fig. 5. (A) Illustration of potential fragmentation pathways of water loss for salbutamol and (B) proposed lowest energy fragmentation pathway, with calculated theoretical thermodynamics.

cleavage of the C–O bond and rearrangement to the shown tropylium structure. Like with the initial water loss, different mechanisms can be considered for the subsequent water loss. The structure postulated for the product ion at *m/z* 148 in the literature was considered [12]; this alternative pathway is shown in Figure S20 but was determined to be less thermodynamically favorable path. The preferred pathway, combined water loss and rearrangement to the tropylium cation was found to be an exothermic process (−32.90 kJ/mol). This exothermicity of the preferred pathway can be used to explain why the *m/z* 148 pathway is experimentally observed (Fig. 4) to initiate at only slightly higher energy than the product ion of the previous step of the dissociation process.

An additional fragment ion at *m/z* 57 could be observed in very low abundance after tuning the instrument specifically for transmission of lower mass product ions (Figure S5). Observance of this diagnostic product ion for beta-2 agonists terminating in a *tert*-butyl group is in agreement with previously reported CID-MS for clenbuterol, terbutaline, and other similar beta-2 agonists [13,32]. A proposed reaction pathway is shown in Figure S19. This pathway assumes direct formation of the *m/z* 57 ion, though loss from the water-loss product ion could also be reasonable. The calculated enthalpy change for this pathway was found to be 209.58 kJ/mol. The large energy barrier for this pathway is consistent with the low relative abundance of this product ion and the requirement of relatively high collision energies to generate it.

3.2.3. Formoterol

Formoterol is another beta-2 agonist, with a more complex structure and, as a result, a more varied dissociation pattern. The energy-resolved CID curves for protonated formoterol are provided

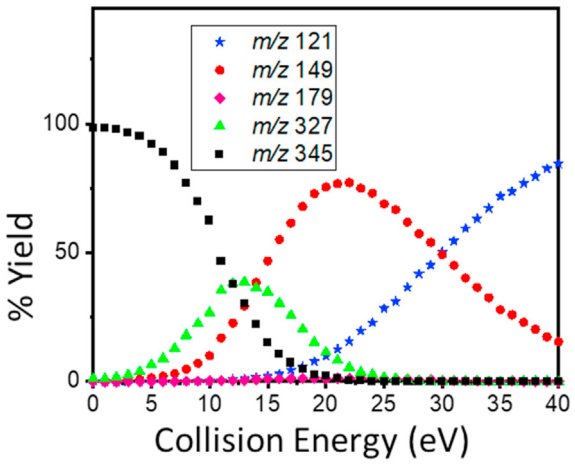

Fig. 6. Energy-resolved CID of protonated formoterol. Black squares represent the precursor ion (m/z 345), green triangles represent the m/z 327 product ion, pink diamonds represent the m/z 179 product ion, red circles represent the m/z 149 product ion, and blue stars represent the m/z 121 product ion.

in Fig. 6 and the proposed dissociation pathways are illustrated in Fig. 7. Figure S14 in the Supporting Information shows an expanded view of Fig. 6 to better illustrate the lower yield product ion *m/z* 179.

Looking at Fig. 6, there are four major dissociation products observed. Consistent with results from salbutamol and isoetharine, initial dissociation proceeds via loss of water, producing an ion at *m/z* 327 (green triangles). The water loss product ion can then dissociate by way of one of two competitive pathways. In the first,

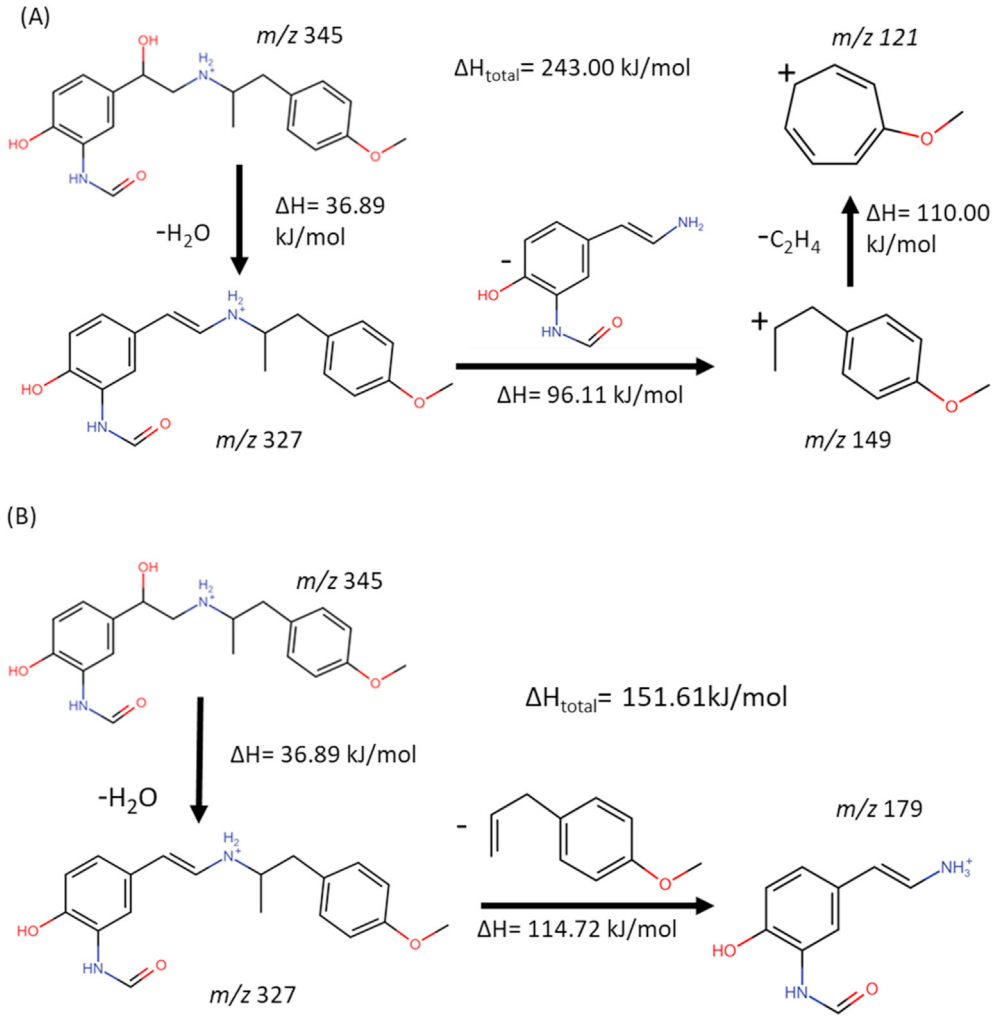

Fig. 7. Proposed lowest energy competitive fragmentation pathways (A and B) for protonated formoterol.

less intense pathway, sequential dissociation via neutral loss of 148 u, tentatively assigned as loss of $C_{10}H_{12}O$, produces the *m/z* 179 ion (pink diamonds). In the second, more prominent competitive pathway, *m/z* 327 ions dissociate further via neutral loss of 178 u, tentatively assigned as loss of $C_9H_{10}N_2O_2$ to form the *m/z* 149 (red circles) product ion. The *m/z* 149 product ion can then further dissociate via neutral loss of 28 u, assigned as loss of C_2H_4, to form the *m/z* 121 product ion (blue stars). Notably, *m/z* 179 and 149 are charge-retention pairs, representing cleavage at the same bond but with alternative product ions and neutral losses based only on which fragment retains the charge. Observance of this pair is consistent with the observance of the *m/z* 57 product ion characteristic of salbutamol, as well. MS^n data are provided in Figure S10, which are consistent with these assignments.

Fig. 7 summarizes the full proposed fragmentation schemes for both competitive pathways with theoretical enthalpies for the most favorable product ion structures considered. Water loss is the initial step in both cases. Given the structure of formoterol, 1,2 and 1,3 elimination were considered, but (consistent with the previous two molecules), 1,2 elimination was found to be thermodynamically preferred (36.89 kJ/mol versus ~94 kJ/mol). From the common precursor of *m/z* 327, cleavage of the C–N bond to form either *m/z* 149 (experimentally more prominent) or *m/z* 179 occurs. For Pathway A, forming *m/z* 149 has an associated theoretical enthalpy change of 96.11 kJ/mol. An alternative rearranged structure for the *m/z* 149 ion was considered, in which a tropylium-like structure was formed, but this pathway was found to be ~13 kJ/mol less favorable. Pathway B represents the charge-retention partner of *m/z* 149 (appearing at *m/z* 179). This step has an associated enthalpy change of 114.72 kJ/mol. Thus, the formation of *m/z* 179 is found to be less favorable than formation of the *m/z* 149 ion. This is consistent with the experimental results (Fig. 6). Pathway A then terminates with cleavage of the C–C bond at the carbocation, forming a primary carbocation, likely accompanied by rearrangement to the tropylium cation, to form *m/z* 121. The calculated theoretical enthalpy change for this final step is found to be 110.00 kJ/mol.

3.2.4. Salmeterol

Salmeterol is the final beta-2 agonist studied herein. Salmeterol has a similar scaffold as the others, however it is significantly larger and has a relatively long chain as part of its structure, making it much more flexible than the other molecules (structure provided in Figure S1) and introducing additional possible dissociation pathways. The energy-resolved CID plot is provided in Fig. 8 and the proposed dissociation pathways are illustrated in Fig. 9.

Looking at Fig. 8, protonated salmeterol produces five major product ions. The initial product ion is observed at *m/z* 398 (pink stars), corresponding to a nominal neutral loss of 18 u, assigned as loss of water, which has consistently been the primary dissociation

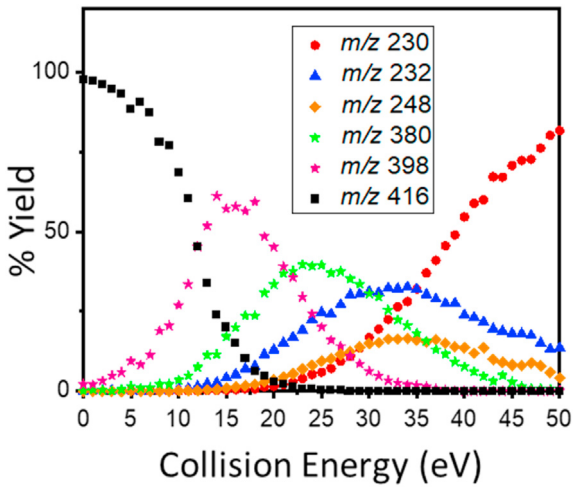

Fig. 8. CID of protonated salmeterol. Black squares represent the precursor ion (m/z 416), pink stars represent the m/z 398 product ion, green stars represent the m/z 380 product ion, orange diamonds represent the m/z 248 product ion, blue triangles represent the m/z 232 product ion, and red circles represent the m/z 230 product ion.

pathway across all four of the molecules discussed herein. The next highest mass product ion is observed at *m/z* 380 (green stars), a nominal neutral loss of 36 u, or a successive loss of 18 u from m/z 398, assigned as loss of a second water molecule. This direct loss of two water molecules prior to any other dissociation is divergent from the results for other molecules studied herein.

From the *m/z* 380 ion, two competitive pathways are proposed. The product ion observed at *m/z* 248 corresponds to a loss of 132 u from the *m/z* 380 product ion, assigned as a loss of $C_{10}H_{12}$. The product ion observed at *m/z* 230 can then be rationalized as successive neutral loss of 18 u from the *m/z* 248 product ion, which is nominally water but for which further investigation of the structures of the previous product ions is warranted to explain its existence (as the original precursor ion structure only has two sites for predicted water loss). Finally, the product ion observed at *m/z* 232 can be assigned as loss of 148 u ($C_{10}H_{12}O$) from the *m/z* 380 ion. MS^n data are provided in Figure S12.

Fig. 9 shows the full proposed sequential fragmentation pathways of salmeterol, with calculated theoretical changes in enthalpies for the pathways consisting of the most favorable structures considered. Initial loss of water is postulated to be β-

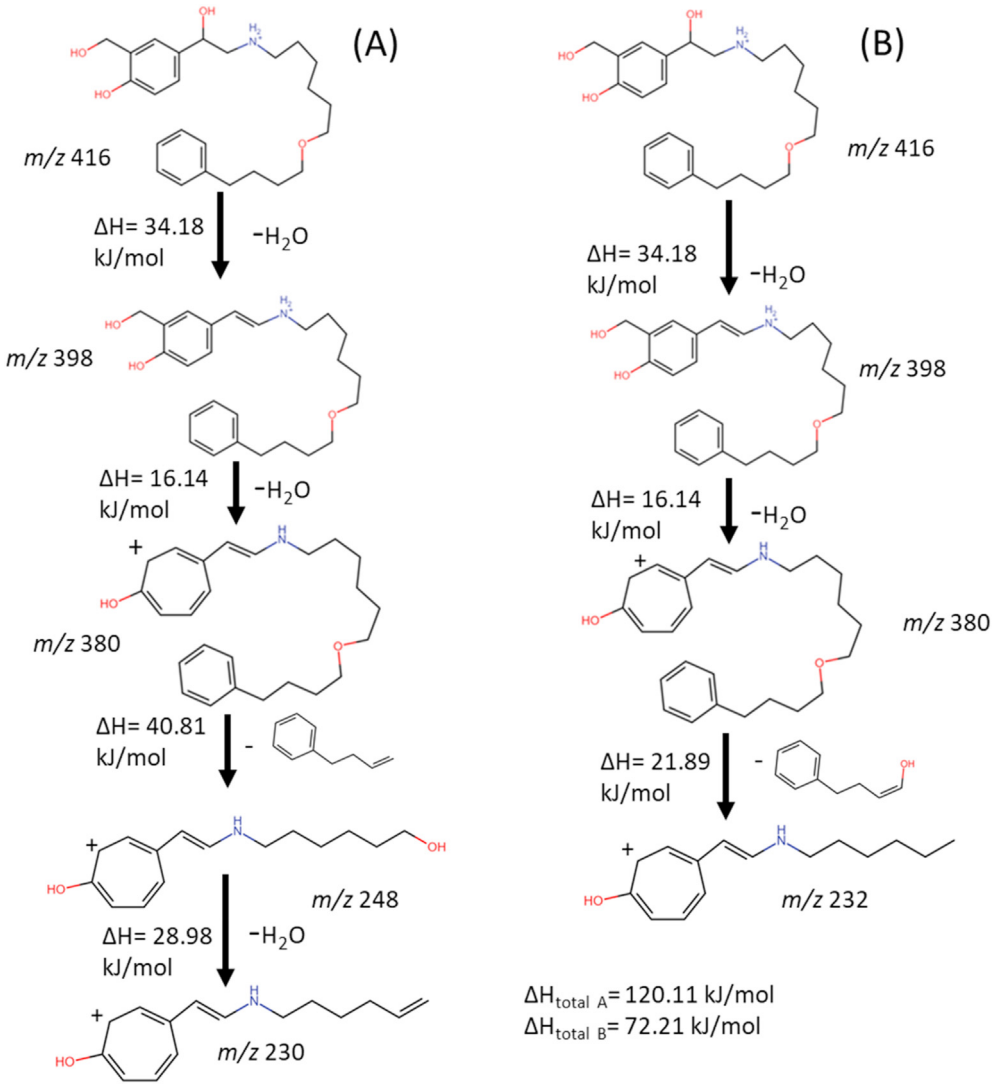

Fig. 9. Proposed lowest energy competitive fragmentation pathways (A and B) of protonated salmeterol, along with mass-to-charge ratios for each ion and theoretical enthalpy changes for each reaction.

elimination of the ethanolamine hydroxyl group, consistent with the proposed pathway for other beta-2 agonists studied, giving rise to the *m/z* 398 product ion (though other water loss pathways were considered, see Figure S22A). The enthalpy change for this step was calculated to be ~34 kJ/mol. This is followed by water loss of the hydroxymethyl substituent of the aromatic ring, similar to the third fragmentation step observed for salbutamol, to form the *m/z* 380 ion (with considered alternative pathways in Figure S22B), with a theoretical enthalpy of reaction of only ~16 kJ/mol. Formation of product ion *m/z* 232 is then postulated to arise from the *m/z* 380 ion, from cleavage of the C–O bond of the ether, with retention of the terminal hydroxyl group on the neutral loss. This pathway has an associated enthalpy of reaction of ~22 kJ/mol. Conversely, O–C cleavage can occur on the other side of the ether, resulting in a product ion with a terminal hydroxyl group, giving rise to the product ion at *m/z* 248 (~41 kJ/mol). It is worth noting here, that the more favorable *m/z* 232 (Pathway B) is also experimentally observed to be in greater abundance than the competitively formed *m/z* 248 (Pathway A). With this newly formed hydroxyl group on the *m/z* 248 ion, additional water loss can occur, explaining the third water loss evidenced by the product ion observed at *m/z* 230.

4. Conclusion

In this work, the dissociation pathways of four beta-2 agonists were explored with energy-resolved CID-MS and complementary DFT thermodynamic calculations. We have observed that loss of water is a common first step of this selection of compounds, where several different mechanisms were postulated and analyzed. Using theoretically calculated thermodynamics, we have proposed product ion structures for all observed product ions (and some hypothetical pathways). These theoretical calculations were then used to rationalize experimental observations (e.g., relative propensity to follow one over the other competitive pathway).

Author statement

Matthew Carlo: conceptualization, methodology, investigation, formal analysis, writing – original draft, visualization; **Peyton York:** formal analysis, investigation, visualization; **Amanda Patrick:** conceptualization, methodology, writing, supervision, project administration, funding acquisition.

Declaration of competing interest

The authors declare that they have no known competing financial interests or personal relationships that could have appeared to influence the work reported in this paper.

Acknowledgements

This work was financially supported by a pilot grant from the Partnership for Clean Competition. Additional support was provided by the Mississippi State University Office of Research and Economic Development Undergraduate Research Program, by the US National Science Foundation Research Experiences for Undergraduates program under Grant # 1852527, and by generous startup funds from Mississippi State University. Computational time and resources were generously provided by the Mississippi Supercomputing Research Center.

Appendix A. Supplementary data

Supplementary data to this article can be found online at https://doi.org/10.1016/j.ijms.2021.116548.

References

[1] M. Johnson, Beta2-adrenoceptors: mechanisms of action of beta2-agonists, Paediatr. Respir. Rev. 2 (2001) 57–62, https://doi.org/10.1053/prrv.2000.0102.
[2] C.K. Billington, R.B. Penn, I.P. Hall, β2 Agonists. Pharmacology and Therapeutics of Asthma and COPD, Springer, 2017.
[3] B. Waldeck, β-Adrenoceptor agonists and asthma—100 years of development, Eur. J. Pharmacol. 445 (2002) 1–12, https://doi.org/10.1016/S0014-2999(02)01728-4.
[4] A.G. Fragkaki, C. Georgakopoulos, S. Sterk, M.W.F. Nielen, Sports doping: emerging designer and therapeutic β2-agonists, Clin. Chim. Acta 425 (2013) 242–258, https://doi.org/10.1016/j.cca.2013.07.031.
[5] K.D. Fitch, β2-Agonists at the olympic games, Clin. Rev. Allergy Immunol. 31 (2006) 259–268, https://doi.org/10.1385/CRIAI:31:2:259.
[6] N.G. Moore, G.G. Pegg, M.N. Sillence, Anabolic effects of the beta 2-adrenoceptor agonist salmeterol are dependent on route of administration, Am. J. Physiol. Metab. 267 (1994) E475–E484, https://doi.org/10.1152/ajpendo.1994.267.3.E475.
[7] The World Anti-doping Code: International Standard: Prohibited List, World Anti-Doping Agency, 2020.
[8] K.B. Joyce, A.E. Jones, R.J. Scott, R.A. Biddlecombe, S. Pleasance, Determination of the enantiomers of salbutamol and its 4-O-sulphate metabolites in biological matrices by chiral liquid chromatography tandem mass spectrometry, Rapid Commun. Mass Spectrom. 12 (1998) 1899–1910, https://doi.org/10.1002/(SICI)1097-0231(19981215)12:23<1899::AID-RCM417>3.0.CO;2-I.
[9] W. Naidong, H. Bu, Y.-L. Chen, W.Z. Shou, X. Jiang, T.D.J. Halls, Simultaneous development of six LC–MS–MS methods for the determination of multiple analytes in human plasma, J. Pharmaceut. Biomed. Anal. 28 (2002) 1115–1126, https://doi.org/10.1016/S0731-7085(02)00002-X.
[10] M. Mazzarino, X. de la Torre, I. Fiacco, C. Pompei, F. Calabrese, F. Botrè, A simplified procedure for the analysis of formoterol in human urine by liquid chromatography–electrospray tandem mass spectrometry: application to the characterization of the metabolic profile and stability of formoterol in urine, J. Chromatogr. B. 931 (2013) 75–83, https://doi.org/10.1016/j.jchromb.2013.05.021.
[11] C. Bozzolino, M. Leporati, F. Gani, C. Ferrero, M. Vincenti, Development and validation of an UHPLC–MS/MS method for β2-agonists quantification in human urine and application to clinical samples, J. Pharmaceut. Biomed. Anal. 150 (2018) 15–24, https://doi.org/10.1016/j.jpba.2017.11.055.
[12] S.H. Chan, W. Lee, M.Z. Asmawi, S.C. Tan, Chiral liquid chromatography–mass spectrometry (LC–MS/MS) method development for the detection of salbutamol in urine samples, J. Chromatogr. B. 1025 (2016) 83–91, https://doi.org/10.1016/j.jchromb.2016.05.015.
[13] M. Thevis, G. Opfermann, W. Schänzer, Liquid chromatography/electrospray ionization tandem mass spectrometric screening and confirmation methods for β2-agonists in human or equine urine, J. Mass Spectrom. 38 (2003) 1197–1206, https://doi.org/10.1002/jms.542.
[14] C. Li, Y.-L. Wu, T. Yang, Y. Zhang, W.-G. Huang-Fu, Simultaneous determination of clenbuterol, salbutamol and ractopamine in milk by reversed-phase liquid chromatography tandem mass spectrometry with isotope dilution, J. Chromatogr., A 1217 (2010) 7873–7877, https://doi.org/10.1016/j.chroma.2010.10.055.
[15] J. Xu, S. Xu, Y. Xiao, K. Chingin, H. Lu, R. Yan, H. Chen, Quantitative determination of bulk molecular concentrations of β-agonists in pork tissue samples by direct internal extractive electrospray ionization-mass spectrometry, Anal. Chem. 89 (2017) 11252–11258, https://doi.org/10.1021/acs.analchem.7b00517.
[16] V.G. Amelin, A.I. Korotkov, A.M. Andoralov, HPLC—high-resolution time-of-flight mass spectrometry: identification and determinarion of β-agonists in food and feed, J. Anal. Chem. 71 (2016) 598–604, https://doi.org/10.1134/S1061934816060034.
[17] E. Zuccato, D. Calamari, M. Natangelo, R. Fanelli, Presence of therapeutic drugs in the environment, Lancet 355 (2000) 1789–1790, https://doi.org/10.1016/S0140-6736(00)02270-4.
[18] E. Zuccato, S. Castiglioni, R. Fanelli, Identification of the pharmaceuticals for human use contaminating the Italian aquatic environment, J. Hazard Mater. 122 (2005) 205–209, https://doi.org/10.1016/j.jhazmat.2005.03.001.
[19] A.R. Depaolini, E. Fattore, F. Cappelli, R. Pellegrino, S. Castiglioni, E. Zuccato, R. Fanelli, E. Davoli, Source discrimination of drug residues in wastewater: the case of salbutamol, J. Chromatogr. B. 1023–1024 (2016) 62–67, https://doi.org/10.1016/j.jchromb.2016.04.033.
[20] H.F. Schröder, W. Gebhardt, M. Thevis, Anabolic, doping, and lifestyle drugs, and selected metabolites in wastewater—detection, quantification, and behaviour monitored by high-resolution MS and MSn before and after sewage treatment, Anal. Bioanal. Chem. 398 (2010) 1207–1229, https://doi.org/10.1007/s00216-010-3958-3.
[21] A. Jelic, M. Gros, A. Ginebreda, R. Cespedes-Sánchez, F. Ventura, M. Petrovic, D. Barcelo, Occurrence, partition and removal of pharmaceuticals in sewage water and sludge during wastewater treatment, Water Res. 45 (2011) 1165–1176, https://doi.org/10.1016/j.watres.2010.11.010.
[22] M. Thevis, D.A. Volmer, Mass spectrometric studies on selective androgen receptor modulators (SARMs) using electron ionization and electrospray ionization/collision-induced dissociation, Eur. J. Mass Spectrom. 24 (2017) 145–156, https://doi.org/10.1177/1469066717731228.

[23] M. Thevis, S. Beuck, S. Höppner, A. Thomas, J. Held, M. Schäfer, J. Oomens, W. Schänzer, Structure elucidation of the diagnostic product ion at m/z 97 derived from androst-4-en-3-one-based steroids by ESI-CID and IRMPD spectroscopy, J. Am. Soc. Mass Spectrom. 23 (2012) 537–546, https://doi.org/10.1021/jasms.8b04236.
[24] J. Moc, J.M. Simmie, H.J. Curran, The elimination of water from a conformationally complex alcohol: a computational study of the gas phase dehydration of n-butanol, J. Mol. Struct. 928 (2009) 149–157, https://doi.org/10.1016/j.molstruc.2009.03.026.
[25] J. Karliner, H. Budzikiewicz, C. Djerassi, Mass spectrometry in structural and stereochemical problems. XCI.1 the electron impact induced elimination of water from 3-hydroxy steroids, J. Org. Chem. 31 (1966) 710–713, https://doi.org/10.1021/jo01341a015.
[26] C. Lifshitz, Tropylium ion formation from toluene: solution of an old problem in organic mass spectrometry, Acc. Chem. Res. 27 (1994) 138–144, https://doi.org/10.1021/ar00041a004.
[27] W.Von E. Doering, L.H. Knox, The cycloheptatrienylium (tropylium) ion, J. Am. Chem. Soc. 76 (1954) 3203–3206, https://doi.org/10.1021/ja01641a027.
[28] P.N. Rylander, S. Meyerson, H.M. Grubb, Organic ions in the gas phase. II. The tropylium ion, J. Am. Chem. Soc. 79 (1957) 842–846, https://doi.org/10.1021/ja01561a016.
[29] M.D. Hanwell, D.E. Curtis, D.C. Lonie, T. Vandermeersch, E. Zurek, G.R. Hutchison, Avogadro : an Advanced Semantic Chemical Editor , Visualization , and Analysis Platform, vols. 1–17, 2012.
[30] A.-R. Allouche, Gabedit—a graphical user interface for computational chemistry softwares, J. Comput. Chem. 32 (2011) 174–182, https://doi.org/10.1002/jcc.21600.
[31] M.J. Frisch, G.W. Trucks, H.B. Schlegel, G.E. Scuseria, M.A. Robb, J.R. Cheeseman, G. Scalmani, V. Barone, G.A. Petersson, H. Nakatsuji, X. Li, M. Caricato, A.V. Marenich, J. Bloino, B.G. Janesko, R. Gomperts, B. Mennucci, D.J. Hratch, Gaussian 16, Revision A.03, 2016.
[32] M. Thevis, Mass Spectrometry in Sports Drug Testing: Characterization of Prohibited Substances and Doping Control Analytical Assays, John Wiley & Sons, Hoboken, New Jersey, 2010.